ISSN: 0974-2115
www.jchps.com Journal of Chemical and Pharmaceutical Sciences

Structural and dielectric studies of Ni^{+2} doped Magnesium Ferrite by Solution Combustion method

Asiya Parveez[1*], Sunar Abdul Khader[2]
[1]Department of Materials Science, University of Mysore, Mysore-570005, Karnataka, India
[2]Department of Physics, Govt. Science College, Chitradurga-577501, Karnataka, India
[*]**Corresponding author: E-Mail: khadersku@gmail.com; Contact number: 919980787658**

ABSTRACT

Nickel doped Magnesium ferrite nanoparticles having the basic composition $Ni_xMg_{1-x}Fe_2O_4$ (x=0, 0.25, 0.5, 0.75, 1) were synthesized using solution combustion method. The structural and dielectric properties of these samples, which are sintered at 800^0C were investigated. The structure and phase of the synthesized samples were probed by X-ray diffraction (XRD) studies. The peaks observed in the XRD spectrum indicated single phase spinel cubic structure for the synthesized Ni^{+2} doped $MgFe_2O_4$ samples. Surface morphology of the samples has been investigated using FESEM. The dielectric constant (ε') and dielectric loss tangent (tan δ) of nano-crystalline Magnesium ferrites were investigated as a function of frequency and Ni^{+2} concentration at 300K, over the frequency range 100 Hz to 1 MHz , using Hioki make LCR Hi-Tester 3250. Frequency dependence of ε' and tan δ is in accordance with the Maxwell-Wagner type interfacial polarization. The electrical conductivity (σ_{ac}) is deduced from the measured dielectric data, and found that the conduction mechanism in the present $Ni_xMg_{1-x}Fe_2O_4$ nanoferrites are in conformity with the electron hopping model.

KEY WORDS: combustion, dielectric, a.c conductivity, Maxwell-Wagner, nanoferrites.

1. INTRODUCTION

Nano-crystalline spinel ferrites are the magnetic oxides which are having excellent electrical and magnetic properties which can be easily tuned by controlling the size of synthesized particles using various synthesis approaches. Because of their imperative technological and bio-medical applications they are employed in numerous devices like radiofrequency circuits, ferro-fluids, hyperthermia, cores of transformer, microwave antennas, magnetic recording (Chavan, 2010; Adam, 2002). With the advent of nanotechnology it is possible to synthesize magnetic oxides in the nano regime and their properties can be modified accordingly (Kulikowski, 1984; Harris, 2009).

Ferrimagnetic materials that are mainly consisting of ferric oxide (Fe_2O_3) are known as ferrites and have spinel cubic structure. They exhibit magnetic hysteresis (M-H curve) and consist of spontaneously magnetized domains. The applications of ferrites depend upon the various magnetic parameters such as saturation magnetization (Ms), Curie temperature (Tc), micro structure, porosity, grain size, etc. The electrical and magnetic properties of spinel ferrites is because of occupancy of cations among the available crystallographic lattice sites such as tetrahedral (A) and octahedral (B) sites (Adam, 2002).

Nickel ferrite belongs to inverse spinel with Ni^{+2} at octahedral (B-site) and Fe^{+3} ions distributed equally in tetrahedral (A-site) and octahedral sites (B-site) (Harris, 2009; Kasapoglu, 2010). Nickel and Magnesium ferrites are used in numerous electronic devices because of their high permeability, high electrical resistivity, mechanical hardness, and chemical stability (Qu, 2006).

Magnesium ferrite is among the technologically important ferrites with spinel cubic structure, which is used in number of application oriented devices such as in field sensors, heterogeneous catalysis, and in gas sensors (Thant, 2010). Recently, structures of nano-magnetic oxides have drawn more attention duo to their tunable material properties that are significantly different when compared to their powders which are at micro level (Liu, 2005; Gul, 2008).

In our present study, samples with the basic composition $Ni_xMg_{1-x}Fe_2O_4$(x=0, 0.25, 0.5, 0.75, 1) were prepared using citrate gel solution- combustion method. This method is involves exothermic and self-propagating thermally-induced reaction of xerogel, obtained from aqueous solutions containing desired metallic nitrates which acts as oxidizer and organic fuel. Stoichiometric proportions between fuel and metallic nitrates are calculated according to the valencies of the reacting elements so as to provide the relation of oxidizer/fuel equal to one. The metallic nitrates are favored as starting materials which are also known as precursors, because of their water-soluble nature, have low ignition temperatures and are easy to prepare.

2. MATERIALS AND METHODS

The $Ni_xMg_{1-x}Fe_2O_4$ nano ferrite (where x=0.0, 0.25, 0.5, 0.75, 1.0) powders were prepared using Solution combustion method. The starting materials are Nickel Nitrate (Ni $(NO_3)_2.6H_2O$), Ferric Nitrate (Fe $(NO_3)_2.9H_2O$), Magnesium Nitrate (Mg $(NO_3)_2$. $6H_2O$, Citric acid ($C_6H_80_7.H_2O$). Here the corresponding aqueous solutions of metallic nitrates and organic fuel (Citric acid) were taken according to stoichiometry. Here, equi-molar citric acid was added into the aqueous solution of metallic nitrates. The aqueous solution containing redox mixture was taken in a silica crucible and is allowed in to a muffle furnace, which was already pre-heated to a temperature of 500^0C.

The mixture finally yields porous and fluffy voluminous powder. The fluffy material was ground to get ferrite powder. The as-burnt ash was calcined at 800^0C for 2 hours to get better crystallization and homogeneous cation distribution in the spinel and finally ground to get Ni-Mg ferrite nano powders.

The structure and phase of the samples were probed by X-ray diffraction (XRD) studies using Bruker AXS D8 Advance X-ray diffractometer (λ=1.5406 A^0). Morphology of the sintered samples has been investigated using Field Emission Scanning Electron Microscope (FESEM, JEOL JSM 6700). The Capacitance, C_p and dissipation factor, tanδ as a function of frequency in the range 100 Hz-1 MHz was studied using a precision Hioki LCR meter-3250. The dielectric constants (ε') and dielectric loss factor (ε'') were determined using the formulae (Kosak, 2004; Maxwell, 1929).

$$\varepsilon' = Ct/\varepsilon_0 A \quad (1)$$

$$\varepsilon'' = \varepsilon' \tan\delta \quad (2)$$

Where, t is the thickness and A the area of the pellet.

The ac conductivity, σ_{ac} was determined from the dielectric loss factor using a relation

$$\sigma_{ac} = \omega\, \varepsilon_0\, \varepsilon'' \quad (3)$$

Where, ε_0 is the vacuum permittivity and $\omega = 2\Pi f$ with f being frequency.

3. RESULTS AND DISCUSSION

Phase and Surface Morphology: The XRD patterns of $Ni_xMg_{1-x}Fe_2O_4$ (where x=0.0, 0.25, 0.5, 0.75, 1.0) system are presented in Figure 1. The presence of (220), (311), (400), (422), (511), (440) and (533) planes in the diffraction patterns confirms the spinel cubic structure for all the sintered samples. From the X-ray diffractogram and XRD data, mean crystallite size was calculated from the most intense peak (311) using the Scherrer's formula, $t=k\lambda/\beta\cos\theta$; where t is crystallite size, β is the full width at half maximum (FWHM) of the peak (311) and k is instrumental constant (Gul, 2008). The calculated average crystallite size is of the range 44-62 nm. From inter-planar spacing (d) and miller indices (hkl) values (Zahi, 2007; Takayama, 2004), the lattice parameters were computed using and are shown in Table 1. Replacement of larger Mg^{+2} cations (ionic radii of Mg^{+2} is $0.72A^0$) with smaller Ni^{+2} ions (ionic radii is $0.69A^0$) causes a decrease in lattice constant.

Microstructures were studied by placing the sintered samples under Scanning electron microscope. The micrographs of the sintered samples are depicted in Fig. 2 (a-c), shows the surface structure for sintered samples of pure $NiFe_2O_4$, $MgFe_2O_4$ and Ni^{+2} doped $MgFe_2O_4$. Optical micrographs show the uniform nature of the particles with some agglomerated grainy structure. The micrographs show the presence of larger grains with a number of interfaces, which further affects, dielectric and magnetic properties of these ferrites.

Dielectric properties: The variation of dielectric constant (ε'), dielectric loss factor (ε'') and ac conductivity (σ_{ac}) with frequency at room temperature for the Pure Magnesium ferrite and nickel doped magnesium ferrite is shown in Fig.3. From the Fig.3 (a), it is clear that ε' decreases at lower frequencies and remains constant at higher frequencies. The variation of dielectric constant with applied frequency is due to charge transport relaxation. The observed dielectric dispersion is attributed to Maxwell and Wagner type interfacial polarization (Wagner, 1913; Maxwell, 1929), as the dielectric constant is a combined effect of dipolar, electronic, ionic and interfacial polarizations. Since ionic polarization decreases with frequency, the measured ε' also decreased with frequency. The higher magnitudes of ε' are related with space charge polarization at grain boundary and heterogeneous dielectric structure. These inhomogeneity arise from synthesis techniques, sintering temperature, impurities, grain structure and pores (Randhawa, 2007; Sutka, 2010). By electron exchange between Fe^{+2} and Fe^{+3}, displacement of electrons takes place with the applied field and these electrons determine polarization. The polarization decreases with increase in frequency and for further increase, the electric exchange between Fe^{+2}/Fe^{+3} cannot follow the alternating field hence reaches the constant value (Randhawa, 2007).

In order to understand the type of charge carriers and type of polarons responsible for conduction, ac conductivity, σ_{ac} were estimated as per $\sigma_{ac} = \omega\, \varepsilon_0\, \varepsilon''$, with ε_0 is the permittivity of free space and $\omega = 2\Pi f$.

The variation of σ_{ac} with frequency, f, is shown in Fig.3 (a-d) for all the five samples. The plots are linear for almost entire range of frequency except at lower frequencies. Linear variation of σ_{ac} with frequency confirms that, conduction in mixed spinel ferrite occurs by the hopping of charge carriers between the localized states which confirms the small polaron type of conduction (Arena, 2008; Lee, 20007). The conduction mechanism in spinel ferrites can be explained based on the hopping of charge carriers between Fe^{+2} and Fe^{+3} ions on octahedral lattice sites. The increase in the frequency of the applied field accelerates the hopping of charge carriers resulting an enhancement in the overall conduction process, thereby increasing the conductivity. At higher frequencies, σ_{ac} remains constant because the hopping frequency of the charge carriers no longer follows the external applied field variations and lags behind it. However, the decrease in conductivity values at lower frequencies can be correlated to conduction by mixed polarons.

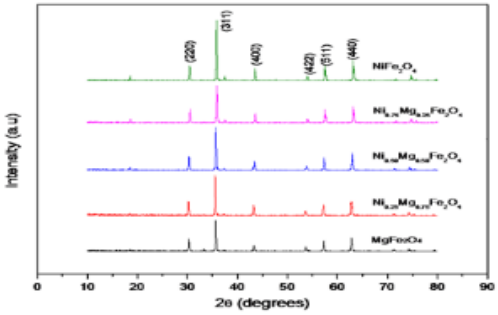

Fig.1. XRD diffractogram for Pure $MgFe_2O_4$ and Ni^{+2} doped $MgFe_2O_4$ samples

Table.1. Lattice constant and Crystallite Size values

Sample	Crystallite size (nm)	Lattice constant 'a' (A^0)
$MgFe_2O_4$	62.30	8.3385
$Ni_{0.25}Mg_{0.75}Fe_2O_4$	47.85	8.3690
$Ni_{0.5}Mg_{0.5}Fe_2O_4$	47.12	8.3300
$Ni_{0.75}Mg_{0.25}Fe_2O_4$	44.88	8.2940
$NiFe_2O_4$	60.04	8.3081

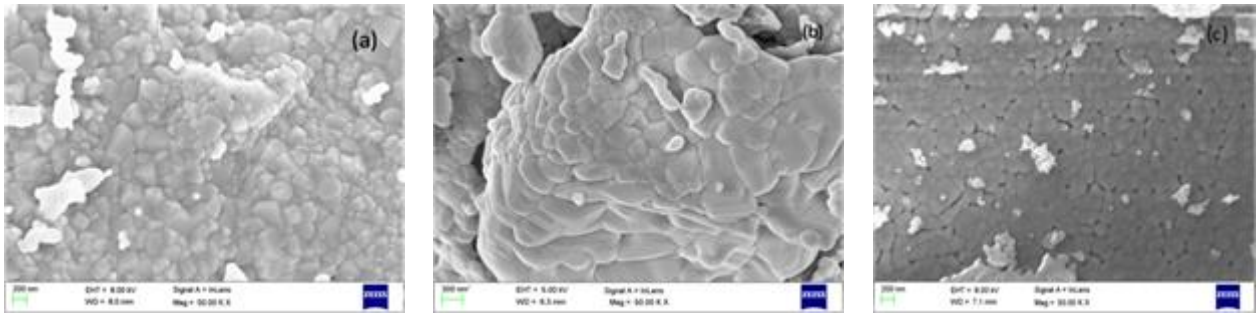

Fig.2. FESEM Micrographs for (a) $NiFe_2O_4$ (b) $MgFe_2O_4$ and (c) $Ni_{0.5}Mg_{0.5}Fe_2O_4$

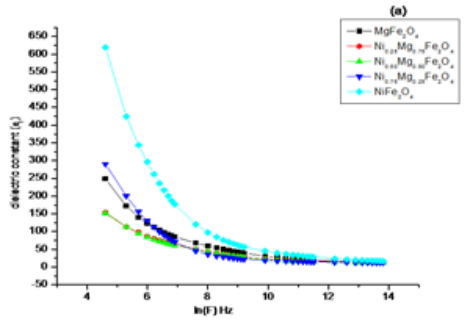

Figure.3 (a). Variation of dielectric constant, ε' with ln(F) at RT

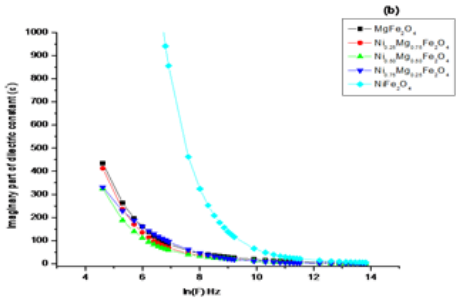

Figure.3(b) Variation of dissipation factor,ε'' with ln(F) at RT

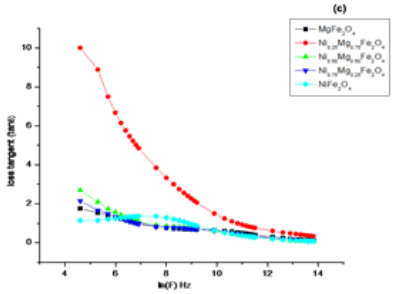

Figure.3(c) Variation of loss factor tanδ with ln(F)

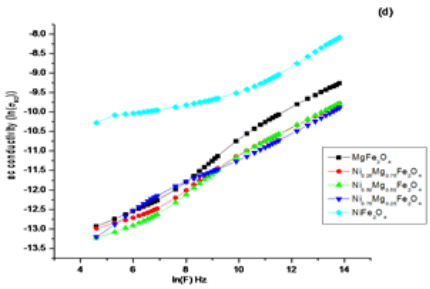

Figure.3(d) Variation of ac conductivity,σ_{ac} with ln(F) at RT

4. CONCLUSIONS

The $Ni_xMg_{1-x}Fe_2O_4$(x=0, 0.25, 0.5, 0.75, 1) samples prepared by solution combustion method exhibited single phase spinel cubic structure. The mean crystallite sizes for the sintered mixed ferrites were calculated using Debye Sherrer formula and are less than 100nm, indicating that the synthesized ferrites are nano in nature. The magnitude of lattice constant for the synthesized samples are in the range of $8.2940A^0$ to $8.3690A^0$. The FESEM results reveals that the morphology of the Ni^{+2}doped $MgFe_2O_4$ nano-particles are nearly spherical in shape. From (ε') V_s ln (F) plots, it is clear that ε' decreases at lower frequencies and remains constant at higher frequencies and ε'' V_s ln (F) resembles the ε' Vs ln (F) curves. From tanδ Vs ln F curves, it is observed that the dielectric loss tangent decreases with increase of frequency and all the sintered samples exhibit low values of loss, which is very essential in designing electronic circuits and applications. The A.C conductivity ln (σ_{ac}) of the synthesized Ni^{+2} doped $MgFe_2O_4$ samples is plotted against ln(F), the plots are linear for almost entire range of frequency except at low frequencies. Linear variation of σ_{ac} with frequency indicates that the electrical conduction occurs because of the hopping of charge carriers between the localized states which confirms the small polaron type of conduction and further it is noticed that along with the Ni^{+2} content the conductivity of doped ferrite also increases. The dielectric dispersion with frequency was observed, and it was explained on the basis of electron-hole hopping mechanism in the light of Maxwell-Wagner two layer models and Koop's theory.

5. ACKNOWLEDGEMENTS

Authors are highly thankful to STIC, Cochin and CENSE, IISc-Bangalore for providing PXRD and FESEM facilities to accomplish this research work.

REFERENCES

Adam J.D, Davis L.E, Dionne G.F, Ferrite devices and materials, IEEE Transactions on microwave theory and Techniques, 50 (3), 2002, 721-737.

Ahmed T.T, Rahman I.Z, Rahman M.A, Study on the properties of copper substituted Ni-Zn ferrites, Journal of Materials Processing Technology, 2004, 153, 797-803.

Aruna S.T, Mukasyas, Combustion synthesis and nano materials, Current opinion in solid state and Material science, 12 (3-4), 2008, 44-50.

Balaji S, Kalai, Selvan K, John Berchmans L, Combustion synthesis and characterization of Sn^{4+} substituted nano-crystalline $NiFe_2O_4$, Materials science and Engineering B, 119 (2), 2005, 119-124.

Chavan S.M, Babrekar M.K, More S.S, Structural and optical properties of nanocrystalline Ni-Zn ferrite thin films, Journal of Alloys and Compounds, 507 (1), 2010, 21-25.

Gul I.H, Ahamed W, Maqsood A, Electrical and Magnetic characterization of nanocrystalline Ni-Zn ferrite synthesis by co precipitation route, Journal of magnetism and magnetic materials, 320, 2008, 270-275.

Harris V.G, Geiler A, Chen Y, Recent advances in processing and applications of microwave ferrites, Journal of Magnetism and Magnetic Materials, 321 (14), 2009, 2035-2047.

Jiao X, Chen D, Hu Y, Hydrothermal synthesis of nano-crystalline $M_x(Zn_{1-x})Fe_2O_4$ (M=Ni, Mn, Cu; x=0.4/0.60) powders, Materials research Bulletin, 37 (9), 2002, 1583-1588.

Kasapoglu N, Birsoz B, Baykal A, Synthesis and magnetic properties of octahedral ferrites, $Ni_xCo_{1-x}Fe_2O_4$ nanocrystals, Central European journal of Chemistry, 5 (2), 2007, 570-580.

Koops CG, Phys Rev, 83:121, 1951.

Kosak A, Makovec D, Znidasec A, Preparation of Mn –Zn ferrite with Micro-emulsion Technique, Journal of European Ceramic Society, 24 (6) 2004, 959-962.

Kulikowski J, Soft magnetic ferrites – development or stagnation, Journal of Magnetism and Magnetic Materials, 41 (1), 1984, 56-62.

Lee S.P, Chen Y.J, Ho C.M, Study on synthesis and characterization of the core shell materials of $Mn_{1-x}Zn_xFe_2O_4$ polyaniline, Jour. Materials science and Engineering B, 143 (1-3), 2007, 1-6.

Liu Y.L, Liu Z.M, Yang Y, Simple synthesis of $MgFe_2O_4$ nanoparticles as gas sensing materials, sensors and Actuators B, Chemical, 107 (2), 2005, 600-604.

Maxwell J.C, Electricity and Magnetism, Vol 1, Oxford University Press, Oxford, 1929.

Mouallem Bahout M, Bertrand S, Pena, Synthesis and Characterization of $Zn_xNi_{1-x}Fe_2O_4$ Spinels prepared by citrate precursor, Journal of solid state chemistry, 178 (4) 2005, 1080-1086.

Qu Y, Yang H, Yang N, The effect of reaction temperature on the particle size, structure and magnetic properties if co-precipitated $CoFe_2O_4$ nanoparticles, Materials Letters, 60, 2006, 3548-3552.

Randhawa B.S, Dosangh H.S, Kumar N, Synthesis of lithium ferrite precursor by combustion method: A comparative study, Journal of Radio Analytical and Nuclear Chemistry, 274 (3), 2007, 581-591.

Sarangi P.P, Vadera S.R, patra M.K, Synthesis and characterization of pure single phase Ni-Zn ferrite nano-powders by oxalate based precursor method, Powder Technology, 203 (2), 2010, 348-353.

Sutka A, Mezinskis G, Ploudons A, Characterization of sol-gel auto-combustion of derived spinel ferrite nano-materials, Power engineering, 56 (3-4), 2010, 44-50.

Takayama A, Okuya M, Kaneko S, Spray pyrolyis deposition of Ni-Zn ferrite thin films, Solid State Ionics, 172 (1-40), 2004, 257-260.

Thakur S, Katyal S.C, Singh M, Structural and Magnetic properties of Nano Ni-Zn ferrite synthesized by reverse micelle technique, Journal of Magnetism and Materials, 321 (1), 2009, 1-7.

Thant AA, Srimala S, Caung P, Low temperature synthesis of $MgFe_2O_4$ soft nanocrystalline ferrite, Journal of Australian Ceramic Society, 46 (1), 2010, 11-14.

Wagner K.W, Ann Phys, 40:817, 1913.

Zahi S, Hashmi M, Daud A.R. Synthesis, Magnetic properties and microstructure of Ni-Zn ferrite by Sol-gel Technique, Journal of Magnetism and Magnetic Materials, 308 (2), 2007, 177-187.